JOPSS
JAEA Originated Papers Searching System

日本原子力研究開発機構機関リポジトリ
Japan Atomic Energy Agency Institutional Repository

Title	Nitrogen K-edge X-ray absorption near edge structure of pyrimidine-containing nucleotides in aqueous solution
Author(s)	Hiroyuki Shimada, Hirotake Minami, Naoto Okuizumi, Ichiro Sakuma, Masatoshi Ukai, Kentaro Fujii, Akinari Yokoya, Yoshihiro Fukuda, and Yuji Saitoh
Citation	Journal of Chemical Physics, 142(17), 175102 (2015)
Text Version	Publisher
URL	http://jolissrch-inter.tokai-sc.jaea.go.jp/search/servlet/search?5051260
DOI	http://dx.doi.org/10.1063/1.4919744
Right	© American Physical Society

Japan Atomic Energy Agency

Nitrogen K-edge x-ray absorption near edge structure of pyrimidine-containing nucleotides in aqueous solution

Hiroyuki Shimada, Hirotake Minami, Naoto Okuizumi, Ichiro Sakuma, Masatoshi Ukai, Kentaro Fujii, Akinari Yokoya, Yoshihiro Fukuda, and Yuji Saitoh

Citation: The Journal of Chemical Physics **142**, 175102 (2015); doi: 10.1063/1.4919744
View online: http://dx.doi.org/10.1063/1.4919744
View Table of Contents: http://scitation.aip.org/content/aip/journal/jcp/142/17?ver=pdfcov
Published by the AIP Publishing

Articles you may be interested in

Nitrogen K-edge X-ray absorption near edge structure (XANES) spectra of purine-containing nucleotides in aqueous solution
J. Chem. Phys. **141**, 055102 (2014); 10.1063/1.4891480

C–C bond unsaturation degree in monosubstituted ferrocenes for molecular electronics investigated by a combined near-edge x-ray absorption fine structure, x-ray photoemission spectroscopy, and density functional theory approach
J. Chem. Phys. **136**, 134308 (2012); 10.1063/1.3698283

Communication: Near edge x-ray absorption fine structure spectroscopy of aqueous adenosine triphosphate at the carbon and nitrogen K-edges
J. Chem. Phys. **133**, 101103 (2010); 10.1063/1.3478548

Pyrimidine and halogenated pyrimidines near edge x-ray absorption fine structure spectra at C and N K-edges: experiment and theory
J. Chem. Phys. **133**, 034302 (2010); 10.1063/1.3442489

Electronic structure of ZnO nanorods studied by angle-dependent x-ray absorption spectroscopy and scanning photoelectron microscopy
Appl. Phys. Lett. **84**, 3462 (2004); 10.1063/1.1737075

Reuse of AIP Publishing content is subject to the terms: https://publishing.aip.org/authors/rights-and-permissions. Downloaded to IP: 133.53.27.54 On: Wed, 10 Aug 2016 07:24:02

Nitrogen K-edge x-ray absorption near edge structure of pyrimidine-containing nucleotides in aqueous solution

Hiroyuki Shimada,[1,a)] Hirotake Minami,[1] Naoto Okuizumi,[1] Ichiro Sakuma,[1] Masatoshi Ukai,[1] Kentaro Fujii,[2] Akinari Yokoya,[2] Yoshihiro Fukuda,[3] and Yuji Saitoh[3]
[1]*Department of Applied Physics, Tokyo University of Agriculture and Technology, Koganei-shi, Tokyo 184-8588, Japan*
[2]*Advanced Science Research Center, Japan Atomic Energy Agency, Tokai-mura, Naka-gun, Ibaraki 319-1195, Japan*
[3]*Synchrotron Radiation Research Center, Japan Atomic Energy Agency, Sayo-gun, Hyogo 679-5148, Japan*

(Received 10 March 2015; accepted 17 April 2015; published online 7 May 2015)

X-ray absorption near edge structure (XANES) was measured at energies around the N K-edge of the pyrimidine-containing nucleotides, cytidine 5′-monophosphate (CMP), 2′-deoxythymidine 5′-monophosphate (dTMP), and uridine 5′-monophosphate (UMP), in aqueous solutions and in dried films under various pH conditions. The features of resonant excitations below the N K-edge in the XANES spectra for CMP, dTMP, and UMP changed depending on the pH of the solutions. The spectral change thus observed is systematically explained by the chemical shift of the core-levels of N atoms in the nucleobase moieties caused by structural changes due to protonation or deprotonation at different proton concentrations. This interpretation is supported by the results of theoretical calculations using density functional theory for the corresponding nucleobases in the neutral and protonated or deprotonated forms. © *2015 AIP Publishing LLC.* [http://dx.doi.org/10.1063/1.4919744]

INTRODUCTION

DNA lesions are induced by ionizing radiation and can cause serious biological effects such as cell death and mutations. DNA lesions can be induced indirectly, by diffusible reactive oxygen species such as OH· radicals produced from irradiated water molecules surrounding the DNA molecule (indirect effect),[1] or can be induced by direct energy transfer from ionizing radiation to the DNA molecule (direct effect). Both pathways are estimated to be almost equally important.[2] The physicochemical mechanism of the direct effect has been studied extensively.[3] However, the mechanism by which the earliest step in the process occurs, namely, the primary formation of base lesions, is not yet well understood, in part because the DNA molecule is in an aqueous environment. For example, Yokoya *et al.* pointed out the importance of hydrating water molecules in the induction of base lesions by the direct effect.[4] Clearly, a detailed investigation of the response of DNA to radiation in an aqueous environment is required.

Monochromatized soft X-rays from synchrotron radiation sources have been used to study the direct effect of radiation and to specify the primary atomic sites (C, N, and O) using inner shell excitation.[5] N atoms are present in only the nucleobases and not in the DNA backbone; therefore, we recently examined the selective excitation of the nucleobase moiety of nucleotides in aqueous solution by measuring the X-ray absorption spectra at energies near the N K-edge.[6–8] Furthermore, because the characteristic binding energies of the 1s electrons of identical atoms are dependent on their bonding sites and their interaction with solvent H_2O molecules, it should be possible to specify the primary site of energy deposition by using X-rays for a particular resonant excitation of the 1s electron to an unoccupied orbital. Detailed measurements of the X-ray absorption near-edge structure (XANES) of DNA and nucleotides should therefore allow precise examination of the primary deposition of radiation energy into a specific atomic site in the nucleobase moiety.

In related previous research,[7,8] we measured the XANES spectra at energies around the N K-edge of nucleotides containing purine derivatives (hereinafter referred to as purine nucleotides), namely, adenosine 5′-monophosphate (AMP), adenosine 5′-triphosphate (ATP), and guanosine 5′-monophosphate (GMP) in aqueous solution. We studied nucleotides instead of bare nucleobases to examine the direct interaction between radiation and the nucleobases moiety because bare nucleobases are insufficiently water soluble to allow XANES measurements on aqueous samples. The XANES spectra were measured at various pH conditions to examine the interaction of the nucleobase moiety with the solvent, and the resonant excitation features in the energy region below the N K-edge (referred to as the pre-edge region) in the XANES spectra were shown to be strongly dependent on the pH conditions. Two characteristic XANES peaks were identified as the core-electron transitions of N atoms with either imine (=N—) or amine (>N—) chemical bonding character. These two types of N atoms are mutually interconverted by protonation and deprotonation (hereinafter jointly referred to as (de)protonation), and this interconversion was observed as the characteristic change in the XANES spectrum.[7,8]

The aim of the present study is to advance further the systematic understanding of how the interaction of the nucleobase

a)Author to whom correspondence should be addressed. Electronic mail: hshimada@cc.tuat.ac.jp

 © 2015 AIP Publishing LLC

Reuse of AIP Publishing content is subject to the terms: https://publishing.aip.org/authors/rights-and-permissions. Downloaded to IP: 133.53.27.54 On: Wed, 10 Aug 2016 07:24:02

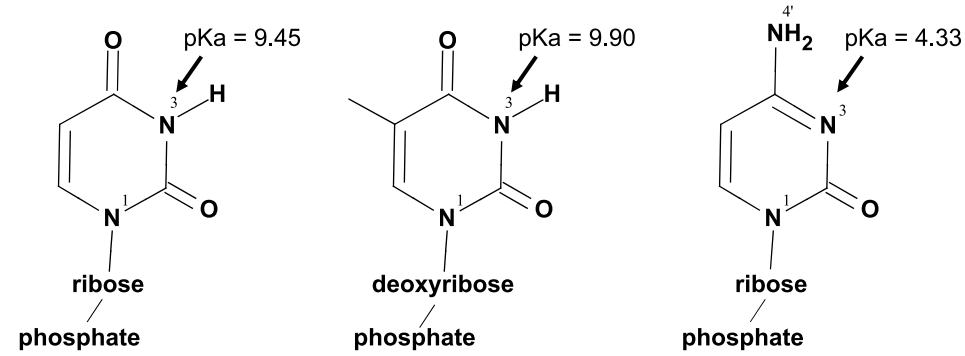

(1) uridine 5'-monophosphate (UMP)

(2) deoxythymidine 5'-monophosphate (dTMP)

(3) cytidine 5'-monophosphate (CMP)

FIG. 1. Structures of the nucleobase moieties of (1) UMP, (2) dTMP, and (3) CMP. The canonical form of each nucleobase is shown, which is the dominant form in an aqueous environment.[9] The structures of uracil, thymine, and cytosine are given by the substitution of a hydrogen atom at the respective N1 atom. The (de)protonation sites (N3) are indicated by arrows together with the (de)protonation pK_a values (taken from Ref. 10).

moiety with the solvent affects the direct radiation interaction. To this end, we measured the XANES spectra in the N K-edge region of three pyrimidine-containing nucleotides (hereinafter referred to as pyrimidine nucleotides), uridine 5′-monophosphate (UMP), 2′-deoxythymidine 5′-monophosphate (dTMP), and cytidine 5′-monophosphate (CMP) (Fig. 1), in aqueous solutions and in films under various pH conditions. The XANES spectra showed a characteristic dependence on the pH of the solution. This dependence is explained by the chemical shift of the core-levels of N atoms caused by (de)protonation. This interpretation is supported by the results of theoretical calculations using density functional theory (DFT). Similarities and differences among the spectra for these pyrimidine derivatives are discussed.

EXPERIMENTAL

Commercially obtained disodium salts of the nucleotides UMP (TCI, Tokyo, Japan and Wako, Osaka, Japan), dTMP (Sigma-Aldrich Japan, Tokyo, Japan), and CMP (Wako, Osaka, Japan) and the nucleobases uracil, thymine, and cytosine (TCI, Tokyo, Japan) were used as received without further purification. UMP disodium salt was dissolved in purified water from a Milli-Q system (Millipore, Tokyo, Japan) to prepare 0.69 mol/l (pH 7.4) and 0.61 mol/l (pH 11.1) solutions for the liquid microjet experiment. The pH values of the solutions were adjusted with 5 mol/l NaOH and were measured using a pH meter (D-51, HORIBA, Kyoto, Japan).

The experiments were performed using beamline BL-23SU[11] at the SPring-8 synchrotron radiation facility in Hyogo, Japan. The experimental setup and procedure were described previously.[7] Briefly, an aqueous solution of UMP is introduced into a vacuum beamline through a 20 μm diameter orifice using a liquid microjet technique[6] and is intersected by a focused beam of monochromatized soft X-rays. The electrons ejected from the intersection region enter the detector vessel though a 1 mm orifice for differential pumping. The electrons are collected by electrostatic lenses and detected by a channel electron multiplier without energy dispersion. The electron yield is normalized by the photon flux obtained from the drain current on the post-focusing mirror at each photon energy and is referred to as the total electron yield. The flux of the soft X-ray is typically around 10^{11} photons/s with a band pass of 0.38 eV (full width at half-maximum; FWHM) at photon energies between 395 and 415 eV. The absolute photon energy is calibrated against two resonant absorption peaks of N_2 molecules in the gas phase with reference energies of 401.10 eV for one of the 1s $\rightarrow \pi^*$ vibrational peaks and 406.15 eV for one of the well-characterized 1s $\rightarrow$ Rydberg state transitions.[12]

The preparation of a CMP solution of sufficient concentration for a liquid microjet experiment is difficult under low pH conditions because of its low solubility. Therefore, dried thin films formed using dilute solutions were used instead. In addition, it was difficult to obtain a sufficient amount of dTMP from a commercial source; therefore, dTMP film samples were prepared in a manner similar to the CMP films. A droplet (~20 μl) of a dilute solution (~1 mmol/l) of CMP or dTMP was placed on a Si plate. Drying under ambient conditions at room temperature produced a film with an area of about 5 mm^2. The samples were placed under vacuum for several hours prior to irradiation to remove residual water and entrapped air. For comparison, films of the nucleobases uracil, thymine, and cytosine were deposited by thermal evaporation of the respective powders onto a Si plate under vacuum. The thickness of the films was controlled to about 100 nm using a quartz oscillator deposition monitor (CRTM-6000, ULVAC, Tokyo). Total electron yields of these film samples were obtained by measuring the emission current from the sample as a function of the photon energy.

CALCULATION

A DFT method was used to calculate the XANES spectra for the canonical form of cytosine and its N3-protonated variant, as well as the canonical form of uracil and thymine and their N3-deprotonated variants (Fig. 1). We considered only the canonical form and not the other tautomeric forms because the canonical forms of the pyrimidine moieties of CMP, dTMP, and UMP are known to be dominant in aqueous solution.[9] All six species (both neutral and (de)protonated CMP, dTMP, and UMP) were assumed to be isolated (i.e., identical to the species in the gas phase). The calculation procedure was basically the same as reported previously.[8] The program package StoBe-DeMon[13] is used for the calculation. The geometries of the molecules were optimized for C_s symmetry and the pyrimidine

Reuse of AIP Publishing content is subject to the terms: https://publishing.aip.org/authors/rights-and-permissions. Downloaded to IP: 133.53.27.54 On: Wed, 10 Aug 2016 07:24:02

ring was assumed to be planar. Under C_s symmetry, molecular orbitals are classified into two irreducible representations, A′ (σ-type) and A″ (π-type). Optimizations were conducted using the BE88 exchange functional[14] and the P86 correlation functional.[15] The triple-zeta valence plus polarization basis sets by Godbout *et al.*[16] in a $(10s6p1d)/[4s3p1d]$ contraction scheme were used for C, N, and O atoms, and a contracted $(5s1p)/[3s1p]$ basis set was used for hydrogen atoms.[13]

The oscillator strengths f_E of discrete excitations of the N 1s electrons are calculated within a framework of the transition potential method[17] using the double basis set technique[18] as previously described.[8] The calculations were performed for each nitrogen atom N1 and N3 for uracil and thymine and additional N4′ for cytosine. The IGLO-III basis functions[19] were used to describe the core-excited N atom, whereas the 1s orbitals of the non-excited N atoms were approximated by effective core potentials. The same functionals for the geometry optimizations were used for calculating f_E. The discrete distributions of f_E obtained by this procedure were convolved with a Gaussian function with a FWHM of 0.7 eV to take into account the vibronic broadening in an approximate manner and were summed for two (uracil and thymine) or three (cytosine) N atoms to yield the theoretical XANES spectra $I(E)$. The ionization potentials IP_{N1s} of the N 1s electrons were obtained using the ΔKS method.[20]

RESULTS AND DISCUSSIONS

Experimental XANES spectra and their pH dependence

The total electron yields for UMP in aqueous solution at pH 11.1 and pH 7.4 around the N K-edge region are shown in Fig. 2. The peak structures are observed in the pre-edge region at about 400-403 eV and are attributed to resonant excitations of 1s electrons of N atoms in the uracil moiety to π^* orbitals; this is discussed in detail below. The electron yields increase at energies above 405 eV, indicating the onset of direct photoionization of the N 1s electrons. In this post-edge region, both yield curves show two broad peaks with local maxima located around 406 eV and 414 eV. Similar structures were observed in the spectrum for pyrimidine in the gas phase and were assigned to resonant excitations to σ^* orbitals.[21]

The fractional contribution to the total electron yields of the constituent atoms was estimated[22] using the atomic cross sections[23] weighted by the known chemical compositions and concentrations of the solutions. These partial contributions are presented in Fig. 2 in the form of stacked areas. The contributions from H atoms are negligible compared with the contributions from the other atoms. The theoretical N 1s ionization thresholds of uracil in the gas phase obtained from the DFT calculations are represented by the step at 406 eV in the N atom cross sections. The experimentally obtained ratio of the yields from N atoms to those from other atoms showed good agreement with the yields estimated from the atomic cross sections. The background contributions from atomic cross sections thus estimated were subtracted from the total electron yields to obtain the XANES spectra for UMP in solution at the N K-edge, as shown in Fig. 3 by curves (1) and (3).

A different procedure for the background subtraction was used for the film samples. The total yield in the energy range from 391 eV to 397 eV below the lowest resonant peak was linearly extrapolated to the higher energy region; this region was regarded as background and subtracted from the total yield.

The XANES spectra of various pyrimidine nucleotides in aqueous solution and in film, as well as of bare nucleobases, are presented in Fig. 3. As described above, all these XANES spectra exhibited isolated or overlapping peaks in the pre-edge region and much broader maxima in the post-edge region. The XANES spectrum (3) obtained for UMP in aqueous solution at pH 7.4 (referred to as "neutral solution" below) shows two nearly overlapping resonant peaks in the pre-edge region, which are labeled E and F. The features in

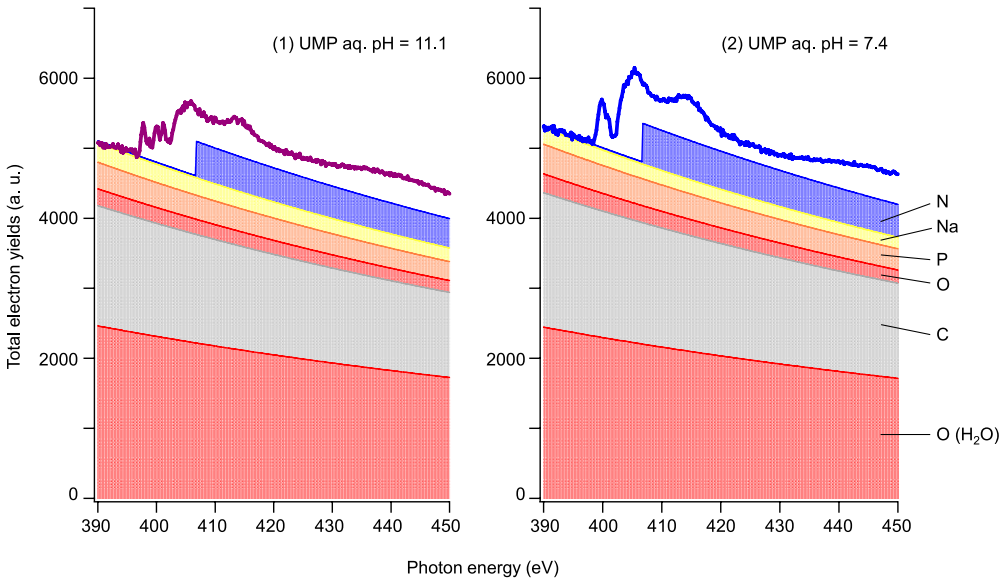

FIG. 2. Total electron yields for UMP in aqueous solution at (1) pH = 11.1 and (2) pH = 7.4. Atomic cross sections weighted with the chemical composition of the solutions are also shown in a stacked layer representation (see text).

Reuse of AIP Publishing content is subject to the terms: https://publishing.aip.org/authors/rights-and-permissions. Downloaded to IP: 133.53.27.54 On: Wed, 10 Aug 2016 07:24:02

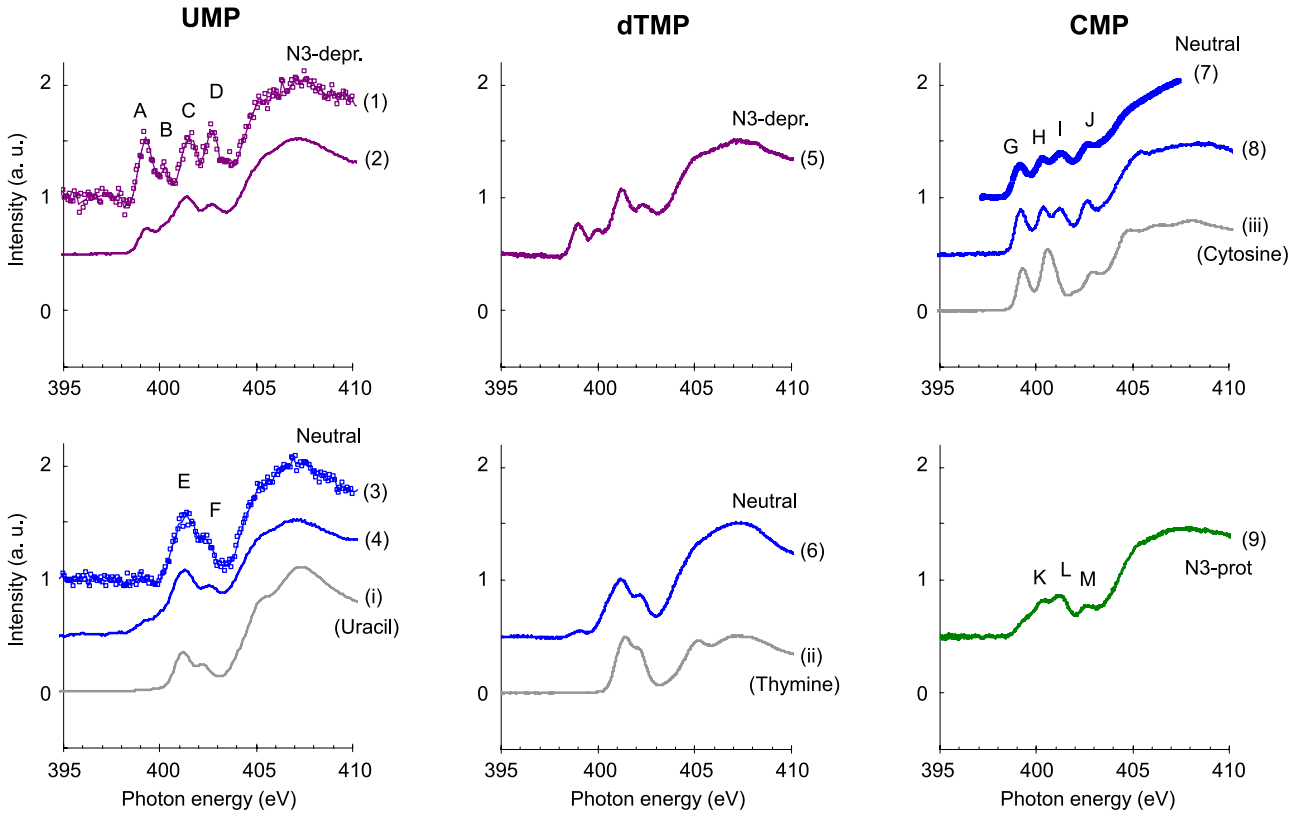

FIG. 3. Experimental N K-edge XANES spectra for pyrimidine nucleotides under different acid/base conditions. N3-deprotonated UMP in aqueous solution (1) and in film (2); neutral UMP in aqueous solution (3) and in film (4); N3-deprotonated (5) and neutral (6) dTMP in film; neutral CMP in aqueous solution (7) (Ref. 6) and in film (8); and N3-protonated CMP in film (9) (see text). The spectra for the corresponding nucleobases uracil (i), thymine (ii), and cytosine (iii) are also shown.

the XANES spectrum (4) for UMP in a dried film prepared using the same aqueous solution are essentially identical to spectrum (3). On the other hand, the XANES spectrum (1) for UMP in basic solution (pH 11.1) is strikingly different from spectra (3) and (4) and shows four clear split resonant peaks in the pre-edge region, which are labeled A, B, C, and D. The XANES spectrum (2) for UMP in a film prepared using the same basic solution shows close similarity to that of (1). In light of previous studies on purine nucleotides,[7,8] the observed differences in the present spectra for UMP in neutral and basic solutions are attributed to a structural difference around a particular N atom in the uracil moiety. The equilibrium constant for deprotonation at the N3 site of UMP is reported to be pK_a = 9.45.[10] Consequently, the N3 atom of UMP in pH 7.4 aqueous solution adopts the structure shown in Fig. 3, whereas the N3 atom is likely deprotonated in aqueous UMP at pH 11.1. Thus, spectra (3) and (4) may correspond to the excitation of the N 1s electrons in the uracil moiety of the canonical form of UMP, while spectra (1) and (2) correspond to those of the N3-deprotonated form. The similarity between spectra (3) and (4) of neutral UMP and spectrum (i) for uracil provides further support that spectra (3) and (4) correspond to the neutral uracil moiety of the canonical form. Finally, the similarity in the XANES spectra for UMP in the aqueous solutions and their dried films suggests that the local environment around the N3 site of UMP in the dried film is similar to that in aqueous solution, as has been shown[7,8] for AMP, ATP, and GMP.

The XANES spectrum (6) in the center panel of Fig. 3 was obtained using a dried film of dTMP prepared from an approximately neutral pH aqueous solution of dTMP. Spectrum (5) is from a dried film prepared from the dTMP solution adjusted to basic pH by the addition of NaOH to the solution used to obtain (6), although the precise pH value is not known. Similar to UMP, a characteristic spectral change was observed in the XANES spectra for dTMP at the two pH conditions. XANES spectrum (6) in the pre-edge region for dTMP film prepared from neutral solution shows two overlapping peaks, while that of spectrum (5) for dTMP film prepared from basic solution shows four distinguishable peaks. This pH-dependent spectral change is similar to the one observed for UMP. As seen in Fig. 1, the structure of the nucleobase moiety of dTMP and UMP is essentially the same except for the presence of a methyl group bound to the C5 atom in dTMP. Consequently, the electronic properties of the thymine moiety in dTMP can be understood similarly to those of uracil in UMP. Moreover, the acid/base properties of dTMP are similar to that of UMP, although the N3 atom of the thymine moiety in dTMP is deprotonated at a higher pH (pK_a = 9.90).[10] Therefore, the similarities in the pH dependence of the XANES spectra between dTMP and UMP indicate that this spectral change is caused by a structural change at the N3 atom in the thymine moiety due to deprotonation. Furthermore, the pre-edge structure of spectrum (6) for dTMP in neutral solution is similar to that of the corresponding nucleobase, thymine (ii).

Reuse of AIP Publishing content is subject to the terms: https://publishing.aip.org/authors/rights-and-permissions. Downloaded to IP: 133.53.27.54 On: Wed, 10 Aug 2016 07:24:02

The right panel of Fig. 3 compares the spectrum (8) of CMP in a film obtained from neutral solution to CMP in aqueous solution (7) reported previously.[6] Both spectra show four resonant peaks in the pre-edge region, labeled G, H, I, and J. The energies of these peaks in spectrum (7) for aqueous solution are almost identical to those for film (8). However, the corresponding spectrum for cytosine film (iii) is somewhat different from those for neutral CMP, as shown in (7) and (8); this is discussed below. Spectrum (9) is of a CMP film prepared using an acidic solution (pH 2.2). Since the pH value of this solution is below $pK_a = 4.33$ for N3 protonation,[10] this spectrum is for the N3-protonated form of CMP. In XANES spectrum (9), three unresolved broader peaks (K, L, and M) are observed which seem to differ from the peak profiles presented in the XANES spectra for both cytosine (iii) and neutral CMP (7) and (8).

The data shown in Fig. 3 demonstrate that an increase in the pH of a pyrimidine solution, i.e., from neutral UMP/dTMP to deprotonated UMP/dTMP, and from protonated CMP to neutral CMP, results in the appearance of new peaks in the lower energy region (398-400 eV). These peaks originate from (de)protonation at the N3 site within the pyrimidine moiety and the consequent change in chemical shift of 1s electrons in N3. The observed systematic similarities between neutral UMP/dTMP and protonated CMP in the lower row of panels in Fig. 3 and between deprotonated UMP/dTMP and neutral CMP in the upper row of panels in Fig. 3 were examined further. Specifically, these experimental spectra were compared with theoretical (calculated) spectra to clarify how structural changes in the pyrimidine moieties induce the N K-edge XANES spectral changes.

Comparison with theoretical spectra: UMP and dTMP

The experimental XANES spectra for pyrimidine nucleotides in aqueous solution and in film were compared with the theoretical spectrum of the corresponding nucleobase in the gas phase. Our purpose was to understand the XANES spectral change in terms of the chemical bonding character of the N atoms in the nucleobase moieties in the neutral and (de)protonated forms and to confirm the above assignment of the spectral changes to structural changes in the pyrimidine moieties. To our knowledge, the XANES spectra $I(E)$ and oscillator strength f_E for only the neutral forms of these pyrimidine nucleobases and nucleotides have been reported.[24,25]

Fig. 4 compares the experimental XANES spectra for UMP and dTMP with the theoretical spectra $I(E)$ for uracil and thymine in the gas phase, respectively. The upper panels show the spectra of the N3-deprotonated species and the lower panels show the spectra of the neutral species. In the present

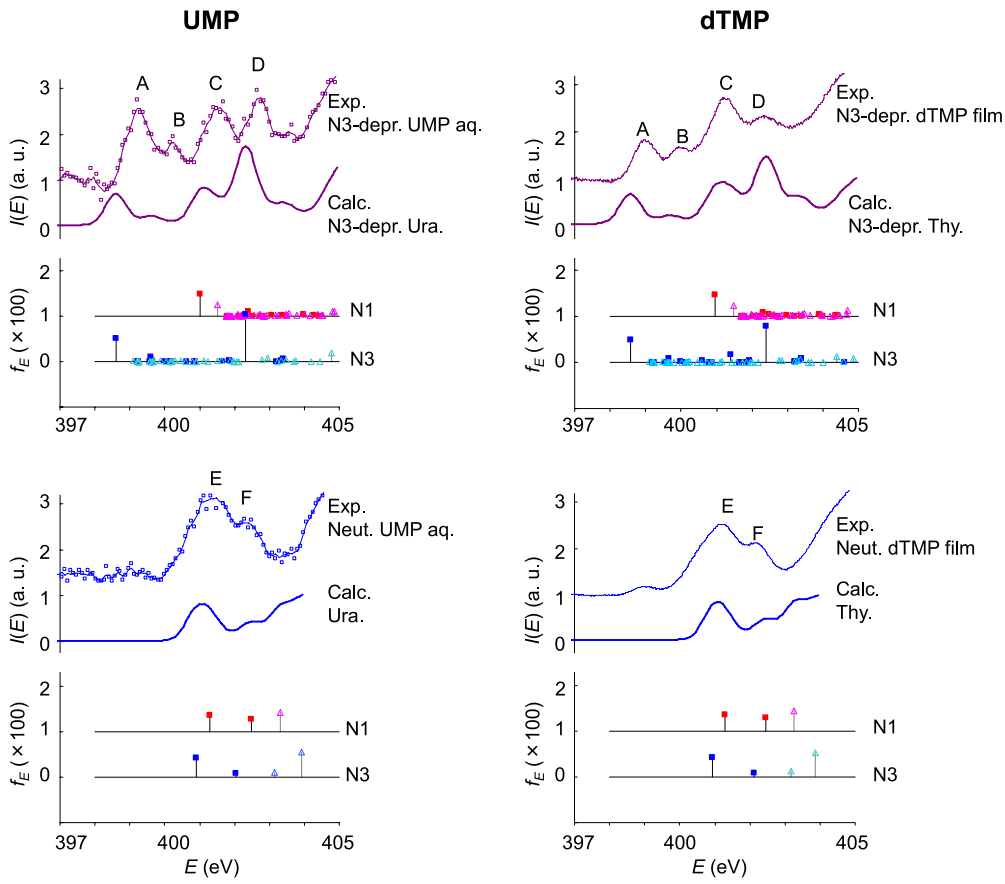

FIG. 4. Comparison of the experimental XANES spectra for UMP in aqueous solution and dTMP in film with theoretical spectra for uracil and thymine in the gas phase. The upper panels show the spectra for N3-deprotonated species and the lower panels show the spectra for neutral species. In each panel, the upper spectrum represents the experimental spectrum for the nucleotide and the central spectrum represents the theoretical spectrum of that nucleobase. The lower part of each panel shows the theoretical oscillator strengths f_E of the 1s electrons of the two N atoms plotted as vertical bars. Filled squares correspond to transitions to π^* orbitals and open triangles to σ^* orbitals.

Reuse of AIP Publishing content is subject to the terms: https://publishing.aip.org/authors/rights-and-permissions. Downloaded to IP: 133.53.27.54 On: Wed, 10 Aug 2016 07:24:02

calculation, the ionization potentials IP_{N1s} of the N 1s electrons in N3-deprotonated uracil and thymine anions obtained using the ΔKS method were about 6 eV lower than those for neutral uracil and thymine. Hence, the energy region around 400 eV for the N3-deprotonated species is embedded in the ionization continuum for the N 1s electrons so that the calculated f_E are quasi-continuously distributed. Similar reductions in IP_{N1s} and overlapping of the ionization continuum with the π* transitions have been observed for the theoretical XANES spectrum of the N1-deprotonated guanine anion.[8]

The theoretical spectra $I(E)$ are in good overall agreement with the experimental spectra. As was pointed out for the experimental spectra, there are no significant differences between the theoretical spectra for neutral uracil and neutral thymine or between their N3-deprotonated species. This is as predicted, since uracil and thymine differ only in thymine having a methyl group at the 5′ position, which does not directly participate in π-conjugation in the pyrimidine ring.

In contrast, the absence of a proton at the N3 position alters the spectra dramatically. To investigate how the proton at the N3 position affects the spectrum, we plotted the theoretical oscillator strengths f_E of the N1 and N3 1s electrons in the lower part of each panel in Fig. 4 as vertical bars. The filled squares represent the transition energies and f_E's of the 1s electrons to π* orbitals and the open triangles the transition energies and f_E's of the 1s → σ* orbitals. The lowest transition energies of N1 1s electrons to the π* orbital are calculated to be approximately 401 eV for uracil and thymine in both their neutral and deprotonated forms, whereas the energies of N3 1s → π* are calculated to be different for the neutral and deprotonated forms. Specifically, the energies of N3 1s → π* for the neutral nucleobases are almost the same as those of N1 1s → π*, whereas the energies for the deprotonated nucleobases are red-shifted by about 2 eV. From these plots, it is apparent that the low energy peaks A and B in the spectra for the N3-deprotonated species are due to transitions of the 1s electrons of deprotonated N3 to π* orbitals.

As reported previously,[7,8] the N K-edge XANES spectra for the purine-containing nucleotides AMP, ATP, and GMP show a systematic change in the relative intensities of the resonant peaks in the pre-edge region upon (de)protonation at the N atoms in the purine moiety. This is ascribed to the specific change in the 1s binding energies of the N atoms, depending on their chemical bonding character.[25–27] The 1s electrons of imine-type (—N=) N atoms are weakly bound, whereas those of amine type (—N<) are strongly bound; for purines, the magnitude of splitting is on the order of several electronvolts. This difference in the N 1s chemical shifts gives rise to the systematic variations in intensities of the resonant peaks for purine nucleotides.[8]

This argument is applicable to the present case of pyrimidine nucleotides. When the uracil and thymine moieties are in the neutral state (i.e., not deprotonated), both the N1 and N3 atoms are amine type (—N<) and their 1s binding energies are almost degenerate. Accordingly, the oscillator strengths f_E of the 1s electrons of the N1 and N3 atoms in the corresponding nucleobases (lower panels in Fig. 4) are located at similar energies. Thus, peaks E and F are assigned to transitions of the 1s electrons of the N1 and N3 atoms to the lowest π_L^* and the second-lowest π_{L+1}^* orbitals, respectively.

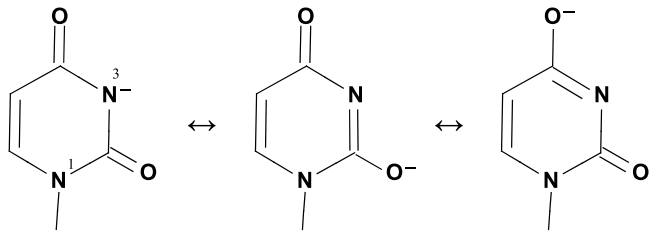

FIG. 5. Possible resonance structures within the uracil moiety of N3-deprotonated UMP.

Once N3 is deprotonated, its chemical bonding character changes from neutral amine type (—N<) to anionic imine type (—N⁻—). Due to π-conjugation, the negative charge on the deprotonated N3 atom can be delocalized over the pyrimidine ring and the N3 atom can take on the character of imine (—N=) type (see Fig. 5 and also Refs. 7 and 8). Thus, the 1s electrons of deprotonated N3 become more weakly bound, and their transition energies are red-shifted by about 2 eV. The lower energy peaks A and B are assigned to transitions of N3 1s electrons to π_L^* and π_{L+1}^*, respectively. Peak C corresponds to the transition of N1 1s electrons to π_L^*. Peak D is dominated by the transition from N3 1s to higher orbitals, with some additional contribution from N1 1s electrons.

We introduced the notation $\{n_i, n_a\}$ for classifying various pyrimidine nucleotides according to the chemical bonding character of their N atoms, where n_i and n_a are the number of N atoms with imine-type and amine-type bonding characters, respectively.[8] Thus, neutral UMP and dTMP are both designated as $\{n_i, n_a\} = \{0, 2\}$, signifying that neutral UMP and dTMP contain no imine N atom and two amine N atoms. Similarly, N3-deprotonated UMP and dTMP are designated as $\{1, 1\}$, indicating that one imine N atom and one amine N atom are present. This classification is used throughout the following discussion and will help clarify several common features of the XANES spectra for the pyrimidine nucleotides UMP, dTMP, and CMP.

Comparison with theoretical spectra: CMP

Let us turn to the XANES spectra for CMP. Fig. 6 compares the experimental spectra for CMP with the theoretical spectra $I(E)$ for cytosine. The upper panel shows the spectra for neutral CMP and neutral cytosine, where one imine (N3) and two amine (N1 and N4′) atoms are present, that is, $\{n_i, n_a\} = \{1, 2\}$. The series of f_E in the upper panel of Fig. 6 shows that while the transition energy of the N3 1s electron to π_L^* is about 399 eV, the transitions of both the N1 and N4′ 1s electrons to the same orbital π_L^* are found around 401 eV and are almost degenerate. This distinction in transition energies is consistent with the fact that N3 is of imine type (—N=), whereas both N1 and N4′ are of amine type (—N<). The corresponding peaks in the experimental XANES spectrum for CMP are tentatively assigned as follows: peak G is the transition of N3 1s electrons to π_L^*, both peaks H and I are the transitions of N1 and N4′ 1s to π_L^*, and peak J is the transition of N3 1s to higher orbitals.

Reuse of AIP Publishing content is subject to the terms: https://publishing.aip.org/authors/rights-and-permissions. Downloaded to IP: 133.53.27.54 On: Wed, 10 Aug 2016 07:24:02

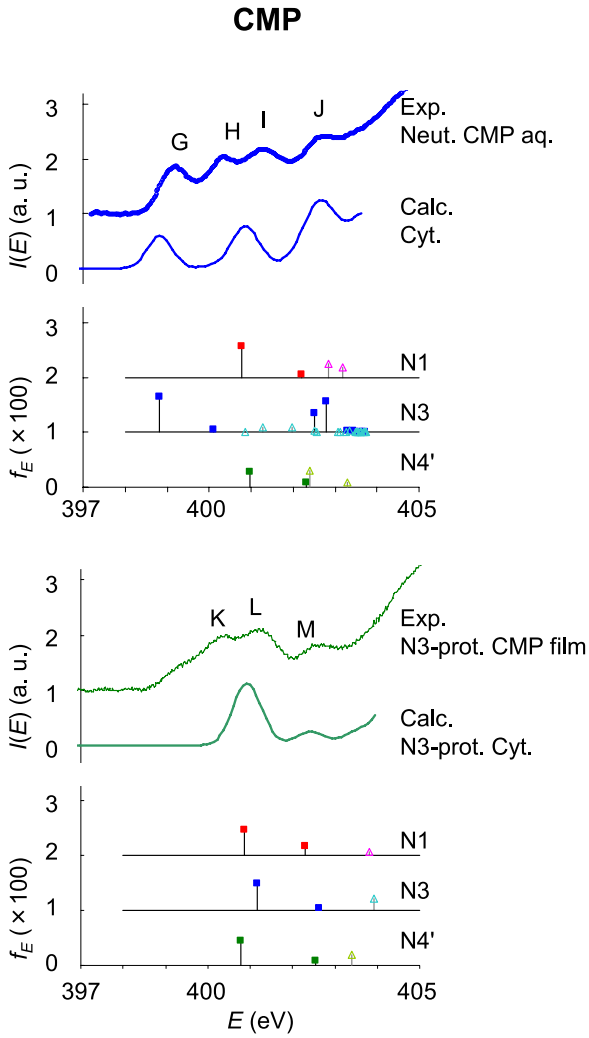

FIG. 6. Comparison of the experimental XANES spectra for CMP with the theoretical spectra for cytosine. The upper panel shows the spectra of neutral species and the lower panel the spectra of N3-protonated species. Theoretical oscillator strengths f_E of the 1s electrons of the three N atoms are also plotted. Symbols are the same as those in Fig. 4.

The spectra for both N3-protonated CMP and cytosine are shown in the lower panel of Fig. 6. Upon protonation, the cationic imine-type (—N^+=) N3 atom can also take on the character of an amine-type (—N<) atom due to π-conjugation (Fig. 7), and thus $\{n_i, n_a\} = \{0,3\}$. Therefore, the 1s → π_L^* transition energy for the protonated N3 atom should be similar to that for the other amine-type N atoms (N1 and N4′). Actually, the series of f_E plotted in the lower panel shows that

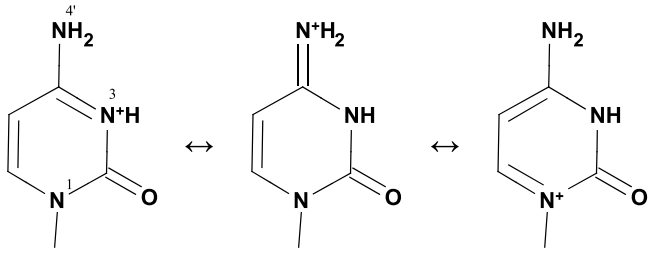

FIG. 7. Possible resonance structures within the cytosine moiety of N3-protonated CMP.

the transitions of N3 1s electrons are blue-shifted by about 2 eV compared to those of neutral CMP and cytosine shown in the upper panel, while those of other N atoms (N1 and N4′) are essentially unchanged. Here, peaks K and L in the experimental spectra, which are not well-resolved, are tentatively assigned to transitions of N1, N3, and N4′ 1s orbitals to π_L^*. Peak M corresponds to transitions of N1, N3, and N4′ 1s orbitals to π_{L+1}^*.

We conclude this discussion of the pH dependence of the XANES spectra for CMP as follows. The protonation of N3 of CMP in acidic solution converts all the N atoms in the cytosine moiety into an equivalent amine type, resulting in the N 1s transitions to the π_L^* orbital becoming essentially degenerate. In contrast, CMP in neutral solution has imine-type N3 and amine-type N1 and N4′ atoms. The presence of the imine N3 atom is reflected in the XANES spectrum as a distinct peak in the low energy region around 399 eV. The agreement between the experimental and theoretical spectra is qualitative; the unidentified origin of the splitting of peaks H and I in the experimental XANES spectrum will be investigated in future work.

General behavior of structural change between UMP, dTMP, and CMP as observed in XANES spectra

Finally, we revisit the similarities among the upper row spectra and the similarities among the lower row spectra in Fig. 3 to help clarify the origin of the systematic features of the spectra. The upper row in Fig. 3 shows the XANES spectra for deprotonated UMP and dTMP, classified as $\{n_i, n_a\} = \{1,1\}$ and neutral CMP, classified as $\{1,2\}$. These species contain one imine N atom. Their spectra (1, 2, 5, 7, and 8 in Fig. 3) are characterized by several distinct resonant peaks in the wide energy range 398-403 eV. In particular, peaks in the lower energy (398-400 eV) region arise from the 1s electrons of these imine N atoms because these electrons are more weakly bound (by about 2 eV) than those of amine N atoms, as mentioned above.

The XANES spectra for neutral UMP and dTMP and for protonated CMP are shown in the lower row of Fig. 3. These species contain no imine N atom and two or three amine N atoms and are classified as $\{n_i, n_a\} = \{0,2\}$ and $\{0,3\}$, respectively. Their spectra (3, 4, 6, and 9 in Fig. 3) are characterized by poorly resolved peaks around 400-402 eV. The absence of an imine N atom in these species results in the absence of peaks in the lower energy (398-400 eV) region.

The similarities among these spectra are clearly explained theoretically by the corresponding plots of the theoretical f_E, as shown in Figs. 4 and 6; that is, the lowest transition energies of all the N1 1s electrons are about 401 eV. In addition, the energy differences between the 1s → π_{L+1}^* and 1s → π_L^* transitions are about 1.3 eV for all these nucleobases; although for deprotonated uracil and thymine, the second-lowest π^*-transitions are not well-defined in the present calculation. The f_E of the N3 1s electrons behave in a similar manner. The transition energies of 1s → π_L^* are about 401 eV for amine-type N3 and are reduced to about 399 eV for imine-type N3. The energy differences between transitions of 1s → π_{L+1}^* and 1s → π_L^* are around 1.2 eV for all these nucleobases. This systematic

Reuse of AIP Publishing content is subject to the terms: https://publishing.aip.org/authors/rights-and-permissions. Downloaded to IP: 133.53.27.54 On: Wed, 10 Aug 2016 07:24:02

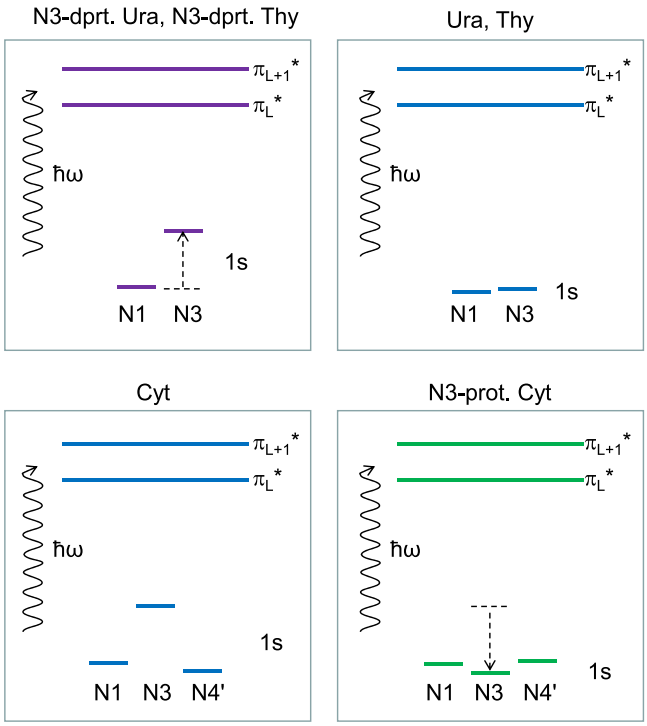

FIG. 8. Schematic electronic states of various pyrimidine nucleobases relevant to the present XANES spectra.

behavior of transition energies across the different pyrimidine nucleobases suggests that the final states, π_L^* and π_{L+1}^*, of the transitions are essentially determined by the pyrimidine ring structure itself, and the effects of the substituents (i.e., differences across uracil, thymine, and cytosine) are small. The electronic states of the pyrimidine nucleobases relevant to the present XANES spectra are depicted in Fig. 8 qualitatively.

To summarize, the XANES spectra for various species of pyrimidine nucleotides shown in Fig. 3 are mainly characterized according to the number $\{n_i, n_a\}$ of imine and amine N atoms. The appearance/disappearance of resonant peaks in the lower energy region (<400 eV) is due to the presence/absence of an imine N atom within the pyrimidine moiety. The physical basis for this characteristic behavior is the bond-dependent chemical shift of N 1s levels and the similarity of π^* orbitals among the pyrimidine nucleobase moieties. A similar classification according to $\{n_i, n_a\}$ has been described for purine nucleotides,[8] where the number $\{n_i, n_a\}$ of imine and amine N atoms is reflected in the relative intensities of two peaks in the pre-edge region. This classification of XANES spectra for both pyrimidine and purine nucleotides provides systematic insights into how a pH-dependent structural change at the nucleobase moiety due to (de)protonation alters the XANES spectrum of the nucleotide.

CONCLUSION

The XANES spectra for the pyrimidine nucleotides CMP, UMP, and dTMP, and their constituent nucleobases, were measured in the N K-edge region in aqueous solution and in films under various pH conditions. The resonant peaks of the 1s electrons of N atoms with different chemical bonding characters, namely, imine type and amine type, appear at different energies, reflecting the difference in the 1s binding energies. A systematic pH-dependence of the XANES spectra was observed and explained by the mutual conversion of imine-type and amine-type N atoms through (de)protonation. Classification of the pyrimidine derivatives by their number of imine-type and amine-type N atoms $\{n_i, n_a\}$ explains well the overall trends of the pre-edge structures in the spectra. For UMP and dTMP, the experimental spectra are reproduced well by the theoretical spectra for nucleobases, with the canonical form in the gas phase calculated using DFT.

The core-excitation process is one starting point for subsequent chemical reaction dynamics in the induction of DNA radiation damage. The core-hole state will de-excite via Auger process, resulting in highly excited states of dication, which will eventually undergo bond breakings and rearrangement reactions. Recently, the significance of direct radiation interaction on the net radiation damage to DNA has been recognized to be almost equivalent to that caused by indirect energy transfer.[2,4,5] The spectroscopic information obtained in this study should aid investigation of the chemical reaction mechanism of the direct effect leading to DNA lesions by identifying the starting point of radiation interaction through site-selective deposition of radiation energy into specific atomic sites in a nucleobase.[8]

The roles of excess H^+ and OH^- produced by irradiated water molecules in inducing base lesions should also be recognized. The present study for pyrimidine nucleotides implies that an excess of H^+ or OH^- ions in the vicinity of nucleotides induces structural change through (de)protonation at the specific N site in the nucleobase moiety and affects the response of nucleotides to radiation. The structural change is a result of a possible indirect effect due to H^+ or OH^- produced during irradiation and results in different effects of direct radiation on the nucleobases or DNA. Although the present measurements were performed under rather extreme H^+ or OH^- concentrations, those ions can be temporally produced in nucleoplasm surrounding DNA during irradiation and affect the interaction of the nucleobase moiety with the solvent. A recent radiation track simulation predicted the existence of an "acid spike;" the pH value of water around a radiation track may be changed as low as 3 that long for several nanoseconds.[28] Under such environments of high proton concentrations, as the present study shows, both geometric and electronic structures of the nucleobase moiety will be affected. Subsequent Auger decay and bond breaking/rearrangement reactions after the production of core-hole states may be different from those under neutral pH conditions. In addition, the reactions involving the attachment of low energy electrons to the nucleobases[29,30] will be affected by these structural changes. The effects of the pH variation these ions on nucleotides during irradiation may provide new insights for a comprehensive understanding of the direct and indirect effects of radiation on hydrated DNA, which may induce damage cooperatively.

ACKNOWLEDGMENTS

This work was supported by JSPS KAKENHI (Grant Nos. 21241017 and 25241010). The experiments at SPring-8 were

Reuse of AIP Publishing content is subject to the terms: https://publishing.aip.org/authors/rights-and-permissions. Downloaded to IP: 133.53.27.54 On: Wed, 10 Aug 2016 07:24:02

carried out under approval of the Japan Synchrotron Radiation Research Institute (JASRI) Proposal Review Committee, Proposal Nos. 2012B3810 and 2013A3810.

[1]P. O'Neill and E. M. Fielden, Adv. Radiat. Biol. **17**, 53 (1993).
[2]D. Becker and M. D. Sevilla, Adv. Radiat. Biol. **17**, 121 (1993).
[3]W. A. Bernhard and D. M. Close, in *Charged Particle and Photon Interaction with Matter*, edited by A. Mozunder and Y. Hatano (CRC Press, Florida, 2004), p. 431.
[4]A. Yokoya, S. M. T. Cunniffe, and P. O'Neill, J. Am. Chem. Soc. **124**, 8859 (2002).
[5]A. Yokoya, K. Fujii, N. Shikazono, and M. Ukai, in *Charged Particle and Photon Interaction with Matter*, edited by Y. Hatano, Y. Katsumura, and A. Mozumder (CRC Press, Florida, 2011), p. 543.
[6]M. Ukai, A. Yokoya, K. Fujii, and Y. Saitoh, Chem. Phys. Lett. **495**, 90 (2010).
[7]H. Shimada, T. Fukao, H. Minami, M. Ukai, K. Fujii, A. Yokoya, Y. Fukuda, and Y. Saitoh, Chem. Phys. Lett. **591**, 137 (2014).
[8]H. Shimada, T. Fukao, H. Minami, M. Ukai, K. Fujii, A. Yokoya, Y. Fukuda, and Y. Saitoh, J. Chem. Phys. **141**, 055102 (2014).
[9]H. Sigel, Pure Appl. Chem. **76**, 1869 (2004).
[10]A. Mucha, B. Knobloch, M. Jeżowska-Bojczuk, H. Kozłowski, and R. K. O. Sigel, Chem. - Eur. J. **14**, 6663 (2008).
[11]Y. Saitoh, Y. Fukuda, Y. Takeda, H. Yamagami, S. Takahashi, Y. Asano, T. Hara, K. Shirasawa, M. Takeuchi, T. Tanaka, and H. Kitamura, J. Synchrotron Radiat. **19**, 388 (2012).
[12]C. T. Chen, Y. Ma, and F. Sette, Phys. Rev. A **40**, 6737 (1989).
[13]K. Hermann, L. G. M. Pettersson, M. E. Casida, C. Daul, A. Goursot, A. Koester, E. Proynov, A. St-Amant, and D. R. Salahub, StoBe-deMon version 3.1, Contributing authors: V. Carravetta, H. Duarte, C. Friedrich, N. Godbout, J. Guan, C. Jamorski, M. Leboeuf, M. Leetmaa, M. Nyberg, S. Patchkovskii, L. Pedocchi, F. Sim, L. Triguero, and A. Vela, 2011.
[14]A. D. Becke, Phys. Rev. A **38**, 3098 (1988).
[15]J. P. Perdew, Phys. Rev. B **33**, 8822 (1986).
[16]N. Godbout, D. R. Salahub, J. Andzelm, and E. Wimmer, Can. J. Chem. **70**, 560 (1992).
[17]J. C. Slater, Adv. Quantum Chem. **6**, 1 (1972); J. C. Slater and K. H. Johnson, Phys. Rev. B **5**, 844 (1972).
[18]H. Ågren, V. Carravetta, O. Vahtras, and L. G. M. Pettersson, Theor. Chem. Acc. **97**, 14 (1997).
[19]W. Kutzelnigg, U. Fleischer, and M. Schindler, *NMR-Basic Principles and Progress* (Springer-Verlag, Heidelberg, 1990).
[20]C. Kolczewski, R. Püttner, O. Plashkevych, H. Ågren, V. Staemmler, M. Martins, G. Snell, A. S. Schlachter, M. Sant'Anna, G. Kaindl, and L. G. M. Pettersson, J. Chem. Phys. **115**, 6426 (2001).
[21]G. Vall-llosera, B. Gao, A. Kivimäki, M. Coreno, J. Álvarez Ruiz, M. de Simone, H. Ågren, and E. Rachlew, J. Chem. Phys. **128**, 044316 (2008).
[22]J. Stöhr, *NEXAFS Spectroscopy* (Springer, Berlin, 1992).
[23]J. J. Yeh and I. Lindau, At. Data Nucl. Data Tables **32**, 1 (1985).
[24]V. Feyer, O. Plekan, R. Richter, M. Coreno, M. de Simone, K. C. Prince, A. B. Trofimov, I. L. Zaytseva, and J. Schirmer, J. Phys. Chem. A **114**, 10270 (2010).
[25]O. Plekan, V. Feyer, R. Richter, M. Coreno, M. de Simone, K. C. Prince, A. B. Trofimov, E. V. Gromov, I. L. Zaytseva, and J. Schirmer, Chem. Phys. **347**, 360 (2008).
[26]V. Feyer, O. Plekan, R. Richter, M. Coreno, G. Vall-llosera, K. C. Prince, A. B. Trofimov, I. L. Zaytseva, T. E. Moskovskaya, E. V. Gromov, and J. Schirmer, J. Phys. Chem. A **113**, 5736 (2009).
[27]F. Wang, Q. Zhua, and E. Ivanova, J. Synchrotron Radiat. **15**, 624 (2008).
[28]V. Kanike, J. Meesungnoen, and J. P. Jay-Gerin, Austin J. Nucl. Med. Radiother. **2**, 1011 (2015).
[29]E. Alizadeh, T. M. Orlando, and L. Sanche, Annu. Rev. Phys. Chem. **66**, 379 (2015).
[30]I. Baccarelli, I. Bald, F. A. Gianturco, E. Illenberger, and J. Kopyrad, Phys. Rep. **508**, 1 (2011).

Reuse of AIP Publishing content is subject to the terms: https://publishing.aip.org/authors/rights-and-permissions. Downloaded to IP: 133.53.27.54 On: Wed, 10 Aug 2016 07:24:02